International Journal of Pressure Vessels and Piping 194 (2021) 104531

Contents lists available at ScienceDirect

International Journal of Pressure Vessels and Piping

journal homepage: www.elsevier.com/locate/ijpvp

Modeling and optimization of A-GTAW process using back propagation neural network and heuristic algorithms

Masoud Azadi Moghaddam, Farhad Kolahan [*]

Ferdowsi University of Mashhad, Department of Mechanical Engineering, Mashhad, Iran

ARTICLE INFO

Keywords:
Activated gas tungsten arc welding (a-GTAW) process
Box-behnken design (BBD)
Back propagation neural network (BPNN)
Particle swarm optimization (PSO) algorithm
And dragonfly algorithm (DFA)

ABSTRACT

Apart from different merits of using conventional gas tungsten arc welding (C-GTAW) process, some demerits have been introduced among which shallow penetration is the most important ones. In order to cope with the mentioned disadvantage, some procedures have been proposed among which using a paste like coating of activating flux during welding process known as activated-GTAW (A-GTAW) is the most extensively used ones. In this study effect of the most important process variables (welding current (C), welding speed (S)) and percentage of activating fluxes (TiO_2 and SiO_2) combination (F) on the most important quality characteristics (depth of penetration (DOP), weld bead width (WBW), and consequently aspect ratio (ASR)) in welding of AISI316L austenite stainless steel parts have been considered. To gather the required data for modeling and optimization purposes, box-behnken design (BBD) in design of experiments (DOE) approach has been used. In order to establish a relation between process input variables and output characteristics, back propagation neural network (BPNN) has been employed results of which have been compared with regression modeling outputs. Particle swarm optimization (PSO) algorithm has been used for determination of BPNN architecture (number of hidden layers and neurons/nodes in each hidden layer). Dragonfly (DFA) and PSO algorithms have been employed for process optimization in such a way that desired AR, minimum WBW, and maximum DOP achieved simultaneously. Finally, confirmation experimental tests have been carried out to evaluate the performance of the proposed method. Based on the results, the proposed procedure is efficient in modeling and optimization (with less than 3% error) of A-GTAW process.

1. Introduction

High quality and surface finish are the major factors considered in using conventional gas tungsten arc welding (C-GTAW) process for fabricating a wide range of alloys including stainless steel, aluminum, titanium and magnesium. Apart from different merits introduced for GTAW process, shallow penetration could be considered as a demerit [1–3]. To tackle the mentioned problem of poor penetration, different procedures have been introduced among which using a paste like coating of activating fluxes on the weld surface before welding process begins, known as activated GTAW (A-GTAW) process is the most important ones [4,5]. In A-GTAW process, a layer of activating flux or fluxes (including oxides, fluorides, and chlorides) on the weld surface before welding process started is coated. During A-GTAW process, depth of penetration (DOP) and consequently weld bead width (WBW) are increased and decreased consequently, due to melting of activating coated flux layer and as a result arc constriction and reversal of Marangoni convection phenomena occurred.

The fluid flow mode of molten metal in weld pool acts as a key factor affecting the weld bead geometry (WBG). Surface tension and consequently the fluid flow are affected by the heat of the welding arc. At the center of the weld pool in comparison with the outer edges, the value of surface tension is smaller. Therefore, a negative surface tension gradient ($(\partial\sigma/\partial T) < 0$) is made [5]. Consequently, an outward movement from the center of the weld pool is resulted based on which a shallow and wide weld pool is made. In A-GTAW process on the top surface of the specimen a paste-like activating flux is covered before the welding process begins. The presence of oxygen, in A-GTAW process acts as a surface active element using which the Marangoni convection is reversed, the surface tension gradient direction changed (a positive value ($(\partial\sigma/\partial T) > 0$) acquired), and consequently the molten metal movement changed from the boundary towards the center of the weld pool (inward movement). This phenomena named as reversal of Marangoni convection which results in an increase in DOP and reduction in

* Corresponding author. P.O. Box 91775-1111.
E-mail address: kolahan@um.ac.ir (F. Kolahan).

https://doi.org/10.1016/j.ijpvp.2021.104531
Received 6 June 2021; Received in revised form 5 August 2021; Accepted 6 August 2021
Available online 11 August 2021
0308-0161/

WBW (Fig. 1) [18].

In C-GTAW process, when the thickness of weldments exceeds 3 mm, a gap between the welding specimens is considered filling which required using filler metal. Whereas, in A-GTAW process specimens of around 8 mm could be fabricated in a single welding pass without considering welding gap, edge preparation, and even using filler metal [6]. There is a great deal of studies in which different aspects of A-GTAW process has been taken into account.

Corrosion behavior, microstructural and mechanical properties of dissimilar welding (AISI316L and P91 steel) have been studied by Vidyarthy et al. [1] considering different activating fluxes. Ramkumar et al. [2] studied the effect of an activating flux in Ti–6Al–4V alloy A-GTAW process on DOP, microstructural and mechanical properties. Based on the results, using activating flux enhances the welding process via increasing DOP and improving mechanical and microstructural properties. Mechanical properties of dissimilar welding of duplex stainless steels and ferrite steels have been studied by Zou et al. [3] using A-GTAW. Based on the acquired results, using A-GTAW process improves mechanical properties in comparison with C-GTAW process. Dissimilar welding of Inconel 800 and Inconel 600 has been studied using C-GTAW and A-GTAW process by Kulkarni et al. [4] In this study, mechanical properties have been considered. Based on the acquired results, an improvement has been reported using A-GTAW process. Furthermore, Microstructural and mechanical properties in fabricating of P91 weldments using A-GTAW process has been studied [5,6]. Process of A-GTAW has been modeled and optimized using response surface methodology (RSM) in order to achieve the largest DOP, by Pamnani et al. [7] Full DOP has been acquired using A-GTAW process in comparison with C-GTAW process [12]. Based on the results, performance of GTAW process could be improved by using activating fluxes (A-GTAW process) by increasing DOP and decreasing WBW simultaneously. Elimination of edge preparation before welding process (for specimens with more than 3 mm thickness) and reduction of welding passes required for accomplishing fabricating in GTAW welding process has been reported by Venkatesan et al. [13] using activating fluxes. Distortion reduction and mechanical properties improvement have been introduced by Chern et al. [14] as the main assets of A-GTAW process. Different fluxes (including oxides, chlorides, and fluorides ones) have been used by Tathgir et al. [15] in dissimilar welding process of stainless steel and low alloy parts in order to improve DOP. Based on the research results, the largest DOP has been reported using oxide fluxes in comparison with other fluxes. However, other fluxes had trivial and negligible effect on DOP.

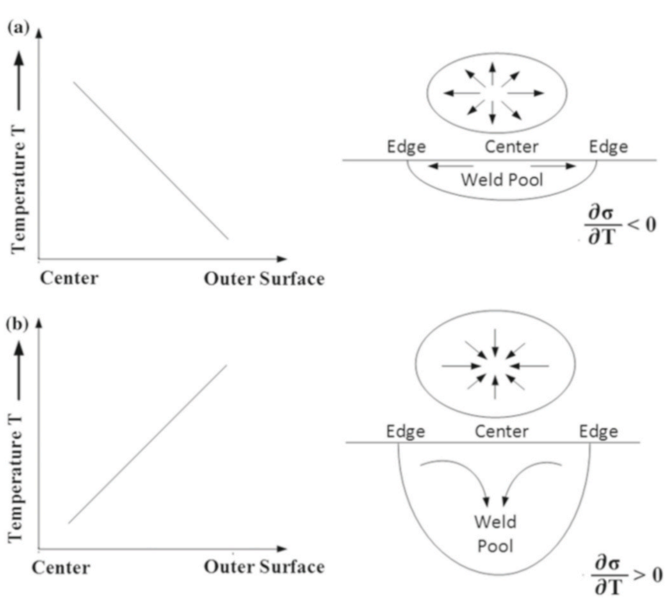

Fig. 1. Schematic illustration of reversal of Marangoni convection phenomena.

Based on the A-GTAW process literature survey, there are different studies in which A-GTAW process have been considered. In these studies, the lack of modeling and optimization of the process senses. To the best of our knowledge, there is no study in which modeling and optimization of A-GTAW process output characteristics (especially DOP, WBW and AR) have been considered simultaneously using BBD-based design of experiments approach, BPNN-based modeling method, and heuristic algorithm-based optimization (DFA and PSO) technique. As different activating fluxes have different effects on WBG, mechanical and metallurgical properties, therefore, in this study effect of combination of the two most crucial activating fluxes has been considered as the process input variable (apart from welding speed and current) and optimized in such a way that DOP increases, WBW decreases and proper value for ASR achieved simultaneously. Based on the preliminary experimental tests carried out using DOE (screening) approach and literature survey studied, as mentioned three process inputs parameters (welding current (I), welding speed (S) and percentage of activating fluxes combination (F)) have been taken into account and their corresponding intervals and levels have been determined. According to the number of process input variables and their predetermined levels, the most appropriate design matrix (BBD) has been considered as the way of carrying out experiments and gathering data required for modeling and optimization purposes. Next, to establish the relations between process input variables (I, S and F) and output characteristics (DOP, WBW and ASR), back propagation neural network (BPNN) has been used. Next, the best BPNN architecture including number of hidden layers and number of nodes/neurons in each hidden layer has been determined using PSO algorithm. Furthermore, results of regression modeling have been used to evaluate the BPNN performance in modeling of the process. Finally, multi-response optimization (in order to achieve desired ASR, maximum DOP and minimum WBW simultaneously) has been carried out using DF and PSO algorithms to determine the values for process input variables. BBD approach has also been used to optimize the process. The proposed approach has been carried out on AISI316L austenitic stainless steel parts. Based on the achieved results, an optimized formula for activating fluxes ($TiO_2 + SiO_2$) has been proposed in such a way a desired ASR with minimum WBW and maximum DOP achieved simultaneously.

2. Experimental set up and equipment used

2.1. Determination of influential process input variables and their corresponding intervals and levels

A-GTAW process is affected by different variables among which, welding current (I) and welding speed (S) are the most influential ones based on the literature review and screening method conducted in this study [1–3]. Furthermore, percentage of activating fluxes combination (F) has been considered as a process input variable to achieve the merits of both in this regard. Similarly, process quality characteristics including DOP, WBW, and ASR are the most important responses of A-GTAW process have been considered to be optimized simultaneously. Welding references have been studied and some preliminary tests (screening method) have been carried out in order to determine the possible working intervals of each process input variable [8–15]. Table 1, lists the

Table 1
A-GTAW process input variables and their corresponding intervals and levels.

Process parameter	Flux combinations (SiO_2–TiO_2)	Welding current	Welding speed
Unit	%	Amps	mm/sec
Symbol	F	C	S
Interval	25–75	100–120	125–175
Level 1	25	100	125
Level 2	50	110	150
Level 3	75	120	175

process input variables and their corresponding intervals and levels based on the screening technique findings. Other input variables with trivial effects have been considered at an optimum fixed level.

To conduct the experimental tests, a DIGITIG 250 AC/DC welding machine has been used (Fig. 1). Furthermore, in this study, Argon (with 99.7% purity) acted as the shielding inert gas.

Experimental tests have been conducted on AISI316L stainless steel specimens with dimension of 100 mm × 50 mm × 5 mm. In this study a combination of Nano oxide fluxes (TiO_2, SiO_2) (+99%, 20–30 nm, amorphous) has been used as activating flux to enhance the welding process. To assure the particle size of activating fluxes, FESEM test has been employed (Fig. 2). In order to prepare a paste-like activating flux coating, prior to welding process begins, 20 g of flux has been mixed for approximately 20 min with 20 ml of a carrier solvent (methanol) using mechanical and magnetic mixers (Fig. 3) [1,2]. Then, the paste like flux was coated on the specimen with a brush and dried before the welding process begins (Fig. 4). When the carrier solvent evaporated, the flux layer remained attached to the surface of the specimen and the welding process could be started.

2.2. Box-behnken design (BBD)

For conducting the experiments required for modeling/optimization purposes a proper matrix of experiments must be determined. Therefore, determination of an appropriate experimental matrix is the next step after selecting the influential process input variables and their corresponding intervals and levels. Generally, to facilitate the identification of the influence of individual process input variables, establish the relationships between process input variables and output responses, and finally determine the optimal levels of input variables in order to get the desired responses (in this study, minimum WBW, maximum DOP, and desired AR), design of experiments (DOE) approach is employed.

In DOE, there are different approaches among which response surface methodology (RSM) due to its merits is the most extensively used ones. There are different RSM designs, including the central composite design (CCD) and its variations (spherical CCD, rotatable CCD, small composite design, etc.), box–behnken design (BBD) and hybrid family of designs (Fig. 5) [20]. In this study, based on the number of input variables and their corresponding levels a BBD's L_{17} matrix has been opted (Table 2).

2.3. Conducting the experiments and measuring the corresponding results

To increase the accuracy of the experimental results, a random order in conducting experiments must have been considered. After welding, three types of process characteristics (DOP, WBW, and ASR) have been taken from each welding sample (Table 2).

For measuring DOP, WBW, and consequently computing ASR, on each sample transverse cross section has been made. Next, to clearly illustrate DOP and WBW, the cut faces were smoothly polished and etched and an optical microscope has been used (Fig. 6). To determine samples' DOP and WBW, images have been consequently processed by MIP (microstructural image processing). Results of the measuring process has been illustrated in Fig. 7.

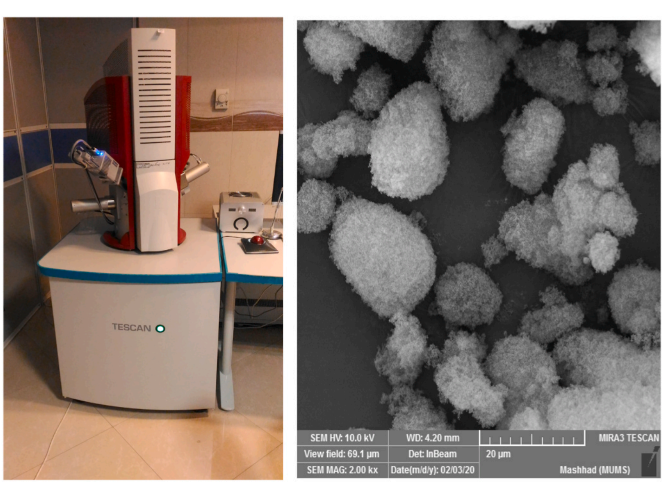

Fig. 2. FESEM test equipment used and results of Nano activating flux (SiO_2) scaling.

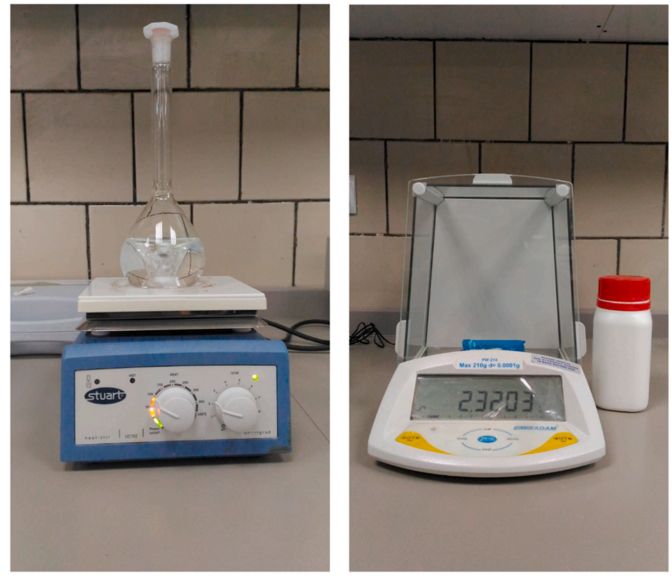

Fig. 3. Magnetic and electronic balance used.

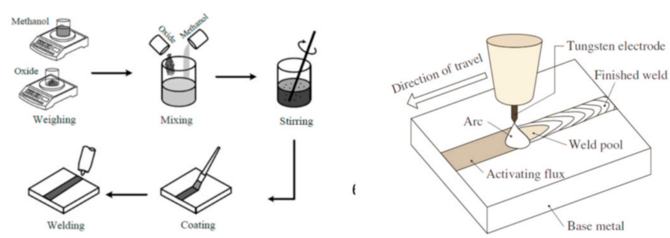

Fig. 4. Schematic illustration of preparation of activating paste-like flux and A-GTAW process.

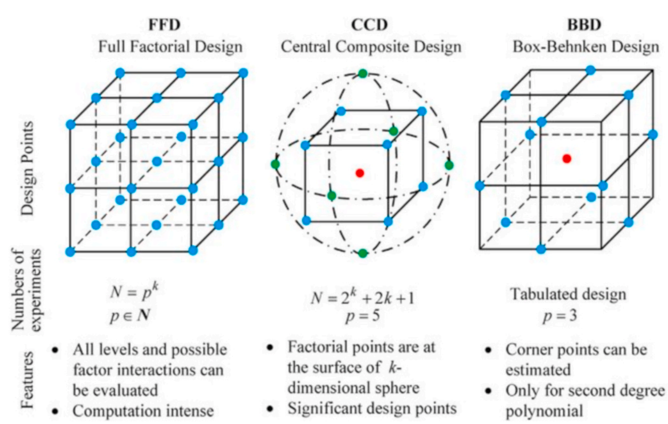

Fig. 5. Schematic illustration of full factorial; central composite and box-behnken designs.

Table 2
Experimental conditions based on BBD and their corresponding measured outputs.

No.	Welding speed (mm/sec)	Welding current (I)	Flux combination (SiO_2 -TiO_2)	Depth of penetration (mm)	Weld bead width (mm)	Aspect ratio (ASR)
1	50	175	100	3.96	6.21	1.57
2	50	150	110	4.65	7.66	1.65
3	50	150	110	5.10	7.58	1.48
4	50	125	120	6.16	6.12	0.99
5	50	125	100	4.84	5.07	1.05
6	75	125	110	5.65	5.74	1.02
7	50	150	110	4.79	8.26	1.72
8	75	150	120	4.95	7.62	1.54
9	50	175	120	4.42	7.64	1.73
10	50	150	110	4.83	7.91	1.64
11	25	125	110	4.58	6.75	1.47
12	75	175	110	3.64	7.82	2.15
13	25	175	110	3.04	7.44	2.44
14	75	150	100	4.03	6.61	1.64
15	50	150	110	4.68	7.96	1.70
16	25	150	120	3.63	7.57	2.08
17	25	150	100	3.15	7.33	2.32

Fig. 6. Optical microscope and electro polish machine used.

3. A-GTAW process modeling

There are several techniques (regression modeling, artificial neural networks, adaptive network fuzzy inference system, and etc.) capable of relating a set of input-output variables among which regression modeling and artificial neural networks (ANNs) especially those coupled with a back propagation algorithm named back propagation neural network (BPNN) are being extensively used ones. In this study modeling of the process has been carried out using regression analysis and BPNN.

3.1. A-GTAW process modeling based on regression analysis

To relate the process input variables to the output responses, regression equations (Equations (1)–(3)) proposed for DOP, WBW, and ASP base on regression modeling and analysis of variance (ANOVA). Tables 3 and 4, represent results of ANOVA for DOP and WBW respectively.

$$DOP = -21.9 + 0.1187 \times F + 0.425 \times C - 0.001189 \times (F \times F) - 0.000189 \times (F \times S) + 0.000435 \times (F \times C) + 0.000251 \times (S \times S) - 0.000879 \times (S \times C) - 0.001251 \times (C \times C) \quad (1)$$

$$WBW = -97.8 - 0.1743 \times F + 0.4264 \times S + 1.338 \times C + 0.000561 \times (F \times S) + 0.000761 \times (F \times C) - 0.001564 \times (S \times S) + 0.000381 \times (S \times C) - 0.00630 \times (C \times C) \quad (2)$$

$$ASR = e^{-6.60} \times F^{-0.2853} \times S^{2.005} \times C^{-0.392} \quad (3)$$

The effect of two main process variables (welding speed and activating flux combination) on the process performance measures (DOP and WBW) has been studied via 3D response surfaces by keeping the rest of the process variable at the constant level. The graphs given in Fig. 8, show the predicted output performance measures depending on the welding speed and activating flux combination. They demonstrate the interaction effect of welding speed and activating flux combination on the measured responses.

3.2. A-GTAW process modeling based on artificial neural networks

Artificial neural networks (ANNs) act as highly complex, nonlinear, parallel processing systems capable of making a relation between a set of input and output parameters. ANNs are embrace of a set of layers (input, hidden and output) in which connecting processing units (neurons/nodes) are organized. An example of a perceptron is shown in Fig. 9 (a), where each input variable (defined as x_i) is related with a weight (w_i) which indicates a portion of the input variable to the neuron for processing. Furthermore, the bias and output signal (parameter) are illustrated by b and y respectively. In this regard, a linear combination of perceptron's inputs applied, obtaining the signal $v = \sum_{i=1}^{N} xi \times wi + b$. furthermore, a transfer function (f) to the signal (v) applied, obtaining the output signal (y). To give the perceptron a nonlinear behavior, sigmoid functions are commonly used as the transfer function [17,18].

Different structures for ANN have been proposed among which multi-layer perceptron (MLP) has been extensively used due to its capability to solve non-linear separable/continuous problems. MLP topology embraces an input layer (including process input variables), hidden layer/s (one or more), and an output layer (including process output characteristics) (Fig. 9 (b)). In the training stage of the ANN procedure a supervised way is employed in order to adjust the weights and biases by providing a set of input and output data pairs allowing the MLP to learn the relationships between input-output parameters (in this study, process input variables and output responses). In back propagation neural network (BPNN) in order to modify the biases and weights of

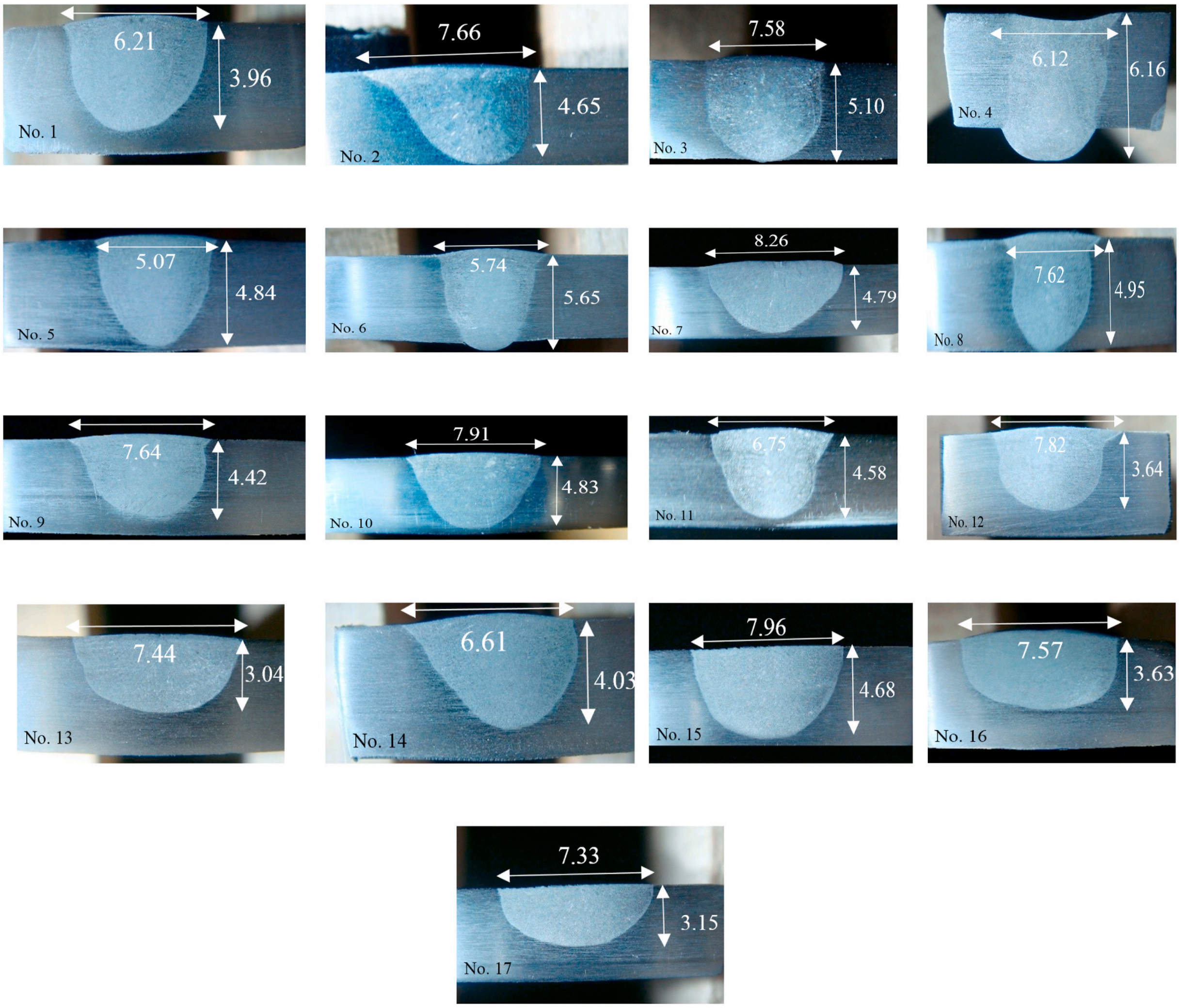

Fig. 7. Cross-sectional profile of weldments.

Table 3
Results of ANOVA for DOP.

Source	Sum of Squares	DF	Mean Square	F-value	p-value	
Model	9.80	5	1.96	71.35	<0.0001	significant
A-F	1.43	1	1.43	51.97	<0.0001	
B–S	4.40	1	4.40	159.97	<0.0001	
C–C	1.47	1	1.47	53.52	<0.0001	
BC	0.1849	1	0.1849	6.73	0.0250	
A^2	2.32	1	2.32	84.53	<0.0001	
Residual	0.3022	11	0.0275			
Lack of Fit	0.1748	7	0.0250	0.7842	0.6355	not significant
Pure Error	0.1274	4	0.0318			
Cor Total	10.10	16				

Table 4
Results of ANOVA for WBW.

Source	Sum of Squares	DF	Mean Square	F-value	p-value	
Model	12.15	6	2.02	30.09	<0.0001	significant
A-F	0.2112	1	0.2112	3.14	0.1068	
B–S	3.69	1	3.69	54.78	<0.0001	
C–C	1.74	1	1.74	25.85	0.0005	
AB	0.4830	1	0.4830	7.18	0.0231	
B^2	4.03	1	4.03	59.93	<0.0001	
C^2	1.69	1	1.69	25.08	0.0005	
Residual	0.6729	10	0.0673			
Lack of Fit	0.3829	6	0.0638	0.8806	0.5774	not significant
Pure Error	0.2899	4	0.0725			
Cor Total	12.82	16				

the MLP, an algorithm (back propagation) in which error of each MLP's input-output pair is calculated and then propagated from the output (process response) layer to the input (process variable) layer is used [15]. The details in this regard are well documented in Refs. [16,19].

Commonly, the architecture of ANN models is determined using trial and error procedure. Whereas, in this study, PSO algorithm has been used to determine the proper BPNN's architecture. The number of hidden layers was diverse from 1 to 3; hence a **3** (number of process input variables)–n_1–n_2–n_3–**3** (number of process output responses) structure was constructed; where n_1, n_2, and n_3 are the number of nodes/neurons for the 1st - 3rd hidden layers respectively. The objective of the training stage is finding an appropriate architecture and weights that leads to minimum error between the real and predicted values.

Fig. 10, shows the variation of mean squared error (MSE) during the training stage of the BPNN model. The performance of the proposed BPNN model has been illustrated in Fig. 11.

Obtaining the best set of A-GTAW process variables to

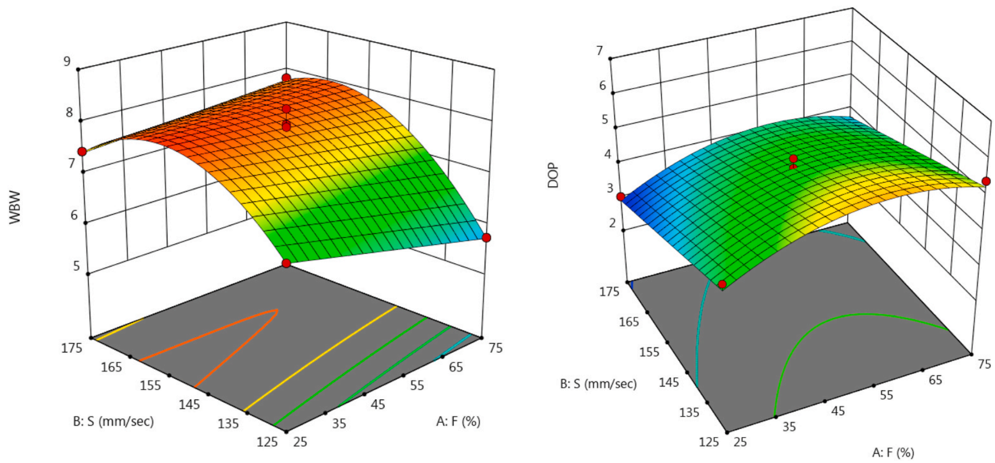

Fig. 8. 3D surface plot of the predicted responses (DOP and WBW) versus welding speed and activating flux.

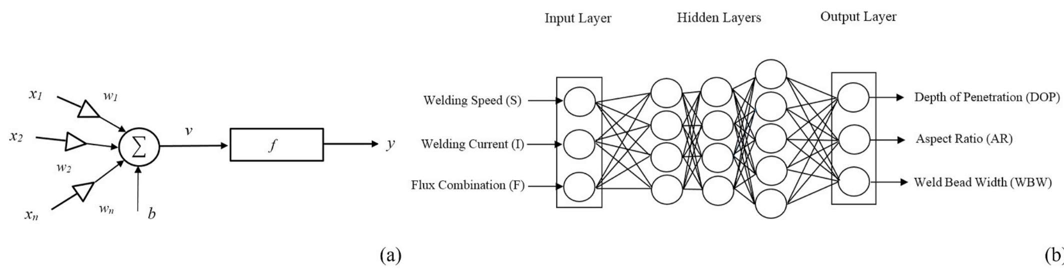

Fig. 9. (a) Example of perceptron and (b) architecture of the proposed BPNN model.

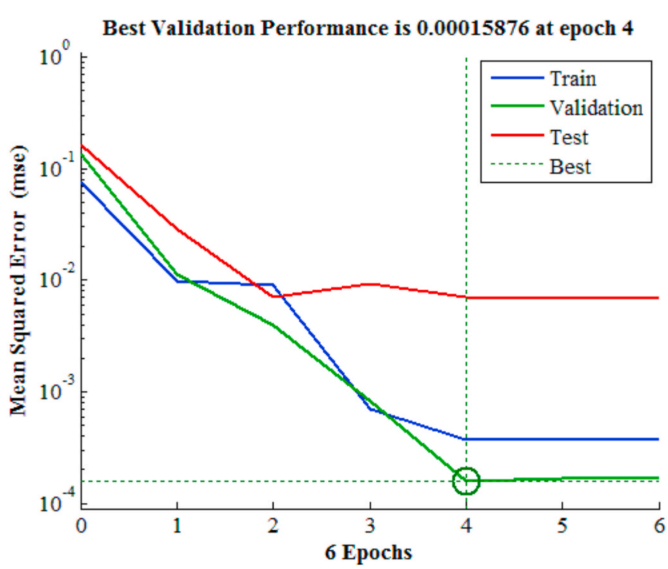

Fig. 10. Variation of mean squared error (MSE).

simultaneously maximize DOP, minimize WBW and attain desired ASR, is the main objective of this study. Consequently, process output measures could be considered together to build a multiple process response in the optimization procedure. Thus, the optimal design can be formulated as a multi-response optimization problem illustrated as Equation (4).

In this study simultaneously achieving high DOP, low WBW, and desired ASR required for multi-criteria optimization. Therefore, process multi-responses are changed into a single measure using Equation (5), where w_1 and w_2 are weighting coefficients to show the importance of DOP and WBW respectively.

$$\text{Maximum DOP} = \text{DOP}(F, I, S),\ \text{Minimum WBW} = -\ \text{WBW}(F, I, S),\ \text{Desired ASR} = [1\text{–}1.4] \quad (4)$$

$$\text{Minimize } F(F, I, S) = (W_1 \times \text{DOP}) - (W_2 \times \text{WBW}),\ (1.0 < AR < 1.4)$$

$$0 < F < 100,\ 90 < I < 130,\ 110 < S < 190 \quad (5)$$

Based on the literature survey which has been confirmed via experimental tests, the weld bead geometry (including DOP, WBW and ASR) has a noticeable influence on solidification cracking and in order to avoid solidification cracks in welding process the best interval for ASR is [1.0–1.4] (Fig. 12) [20].

In Fig. 13 the comparison between regression and BPNN prediction has been carried out. Based on the acquired results, BPNN model (with less than 3% error) is more efficient than the regression based model (with about 12% error) for modeling of the process.

4. An introduction to heuristic algorithms

Nowadays, different heuristic algorithms for different optimization purposes have been proposed (including ant colony (AC), genetic algorithm (GA), bee colony (BC), tabu search (TS), simulated annealing (SA), particle swarm optimization (PSO), dragonfly (DF), and etc.) among which DF and PSO, based on their merits are being extensively used. Few input parameters to adjust (easy programming) and fast convergence are the major advantages of PSO algorithm. DFA is employed for optimization of a wide range of problems in different research areas (simple and easy to implement). Moreover, having few parameters for tuning, reasonable time of convergence are other merits of DFA over other heuristic algorithms.

Based on the mentioned reasons DF and PSO algorithms have been considered as the heuristic algorithms to optimize A-GTAW process variables in order to achieve maximum DOP, minimum WBW and

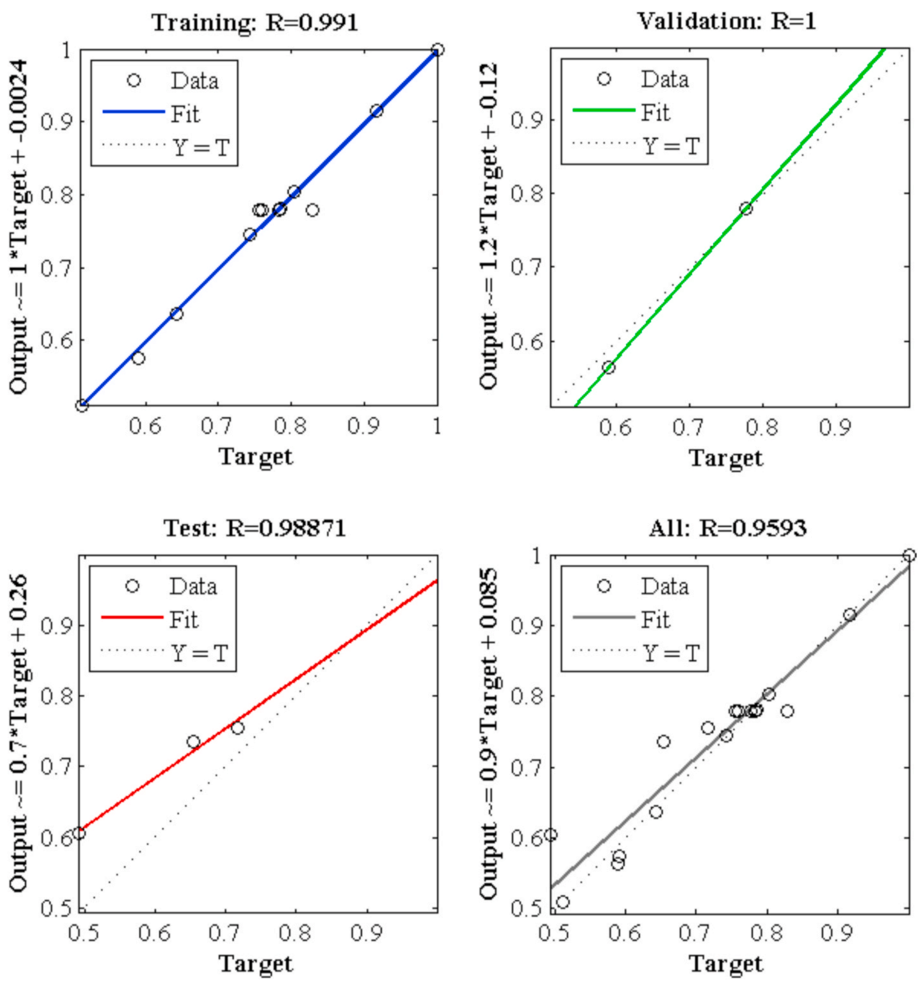

Fig. 11. Performance of the proposed BPNN model in training, validation and test stages.

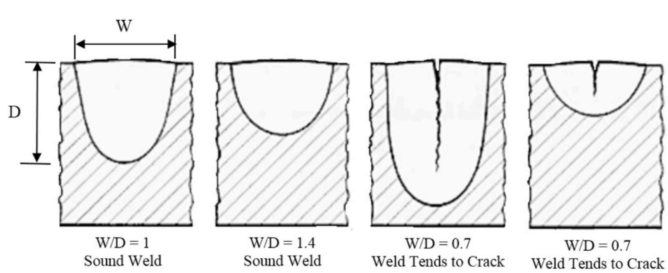

Fig. 12. Effect of ASR values on tendency of occurring solidification cracks.

desired value of ASR simultaneously. The details of these algorithms' procedures are well documented in Ref. [19].

4.1. Particle swarm optimization algorithm

Particle swarm optimization (PSO) is a random-generated and population-based evolutionary heuristic algorithm proposed by Kennedy and Eberhart [21]. First, a population of random solutions initialized and generations for optimum searching updating. Next, the current optimum solutions (called particles) followed by potential particles through the problem space. The best solution achieved and the corresponding location obtained named "pBest" and "gBest" respectively. The PSO algorithm procedure comprises changing the velocity of each particle toward its "pBest" and "gBest". Acceleration toward "pBest" and "gBest" is being done using a random term with separate random numbers for weighing velocity generated. For updating the particles, the following equations (6) and (7) are employed [22–24].

$$V_{i+1} = w \times V_i + C_1 \times r_i \times (pBest_i - X_i) + C_2 \times r_i \times (gBest_i - X_i) \tag{6}$$

$$X_{i+1} = X_i + V_{i+1} \tag{7}$$

Where, for each potential solution/particle, the term V_{i+1} is determined based on its previous velocity (V_i), global best location and best solution (gBest and pBest). The terms "r_1" and "r_2" are generated in the range of [0, 1] randomly. In order to pull each particle/solution towards global best location and best solution, acceleration constants ("c_l" and"c_2") are used. The individual particle's position (X_i) in solution is being updated using Equation (7) [25–28].

The term "w" (inertia weight) plays an important role in the algorithm convergence behavior. In order to explore the design space globally, the large amount of inertia weights selected. While, small amount of inertia weights results in concentrating the velocity updates to nearby regions of the design space [25].

However, the architecture of BPNN is determined conventionally using trial and error, in this study the PSO algorithm has been employed to determine the number of hidden layers of BPNN architecture and nods in this layers. The performance of each evolutionary algorithm is affected by its own distinctive tuning variables. The details of the PSO procedure are well documented in Refs. [20–24].

The adjusting parameters used for controlling PSO algorithm has been carried out as the following.

PSO variables: Population: 50; Number of iteration performed: 150; Learning factor c_1 and c_2: 2.

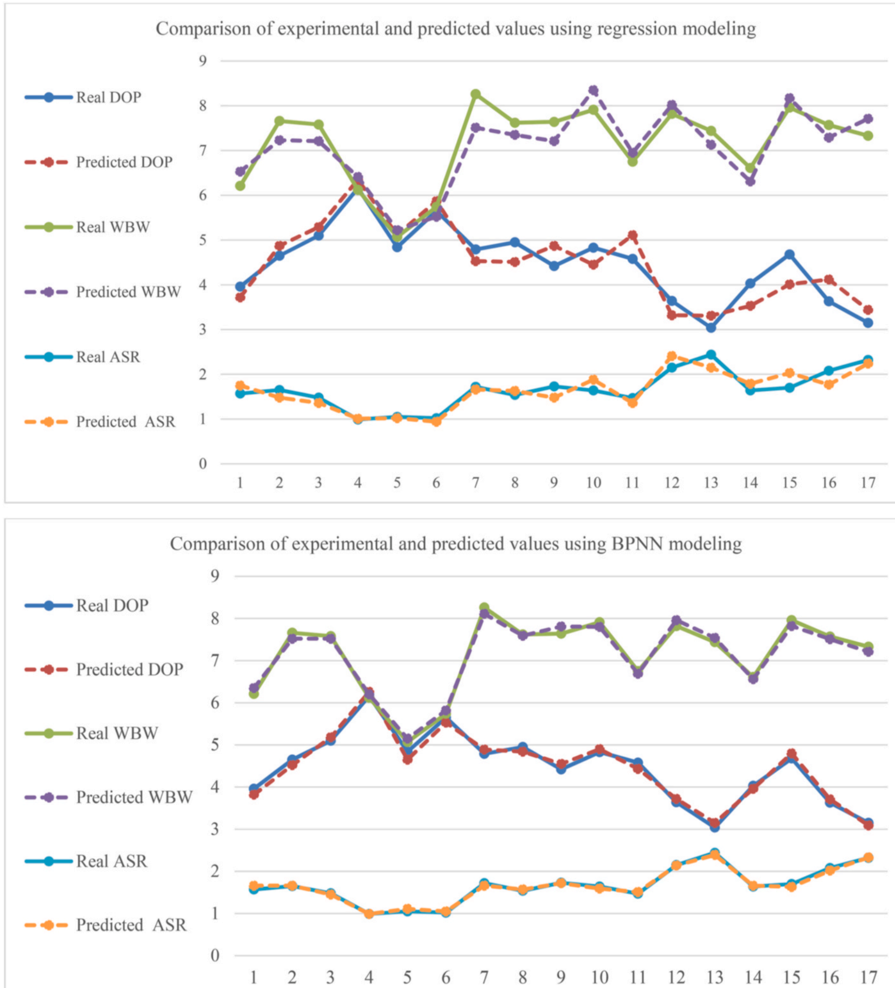

Fig. 13. Comparison of experimental and predicted values using regression and BPNN modeling.

The main objective of the training stage of a BPNN is finding an appropriate architecture and proper values for network weights that leads to minimum error between the real and predicted outputs. A **3–4–4–5–3** architecture (Fig. 9 (b)) results in the best interpolation performance and less MSE value using PSO algorithm. Table 5, represents only a set of architectures has been proposed by PSO algorithm, among which the last is the most appropriate one. The optimized parameters of BPNN model using PSO algorithm has been illustrated in Table 6.

Table 6
BPNN model's parameters based on PSO algorithm optimization.

BPNN Parameter	Value		
Number of hidden layers	1	2	3
Number of hidden layers' neurons	4	4	5
Coefficient of transfer functions For hidden layer	1		
For output layer	1		
Learning rate	0.1		
Momentum constant	0.5		
Screen update rate	100		
Number of iterations	500		

4.2. *Dragonfly algorithm*

Dragonflies are small insects which hunt marine insects and even small fishes and their unique swarming behavior is interesting fact about them. Hunting and migration are the two main purposes of swarm which has been carried out by dragonflies. The hunting is called static/feeding swarm in which dragonflies make small groups and hunt other flying insects. The key characteristics of a static swarm are local movements and sudden changes in the flying path [29].

Table 5
Performance of training different network architectures.

Network architecture	MSE	R^2
3-2-2-2-3	0.03242	0.9906
3-3-2-2-3	0.04631	0.9910
3-3-3-3-3	0.05212	0.9924
3-4-3-3-3	0.08431	0.9931
3-4-4-4-3	0.00391	0.9943
3-4-4-5-3	0.00463	0.9959

The migration is called dynamic/migratory swarm in which an enormous number of dragonflies make the swarm for migrating [30].

The two mentioned swarming behaviors (hunting and migration) are reminiscent of exploration and exploitation in optimization procedure using heuristic algorithms. The main objective of the exploration phase is creating sub-swarms and fly over different areas in a static swarm, which is carried out by dragonflies. In the exploitation phase, dragonflies fly in bigger swarms and along one direction.

Separation (static avoidance of the individuals from other individuals), alignment (velocity matching of individuals to that of other individuals), and cohesion (tendency of individuals towards the center of the mass of the neighborhood) are three basic principles of swarms' behavior.

Survival is the main objective of any swarm, so all of the individuals should be distracted outward enemies and attracted towards food sources considering of which five main factors in individuals position updating in swarms required. The stated behaviors are modeled mathematically as follows:

The separation, alignment, attraction towards a food source, and distraction outwards an enemy are calculated using Equations (8)–(12) respectively.

$$S_i = -\sum_{j=1}^{N} (X + X_j) \tag{8}$$

$$A_i = \frac{\sum_{j=1}^{N} V_j}{N} \tag{9}$$

$$C_i = \frac{\sum_{j=1}^{N} X_j}{N} - X \tag{10}$$

$$F_i = X^+ - X \tag{11}$$

$$E_i = X^- + X \tag{12}$$

Combination of these five corrective patterns could be assumed as the behavior of dragonflies. In this regard, two vectors (step (ΔX) and position (X)) have been considered to update the position and simulate movements of dragonflies respectively. The step vector displays the dragonflies movement direction and defines as Equation (13):

$$\Delta X_{t+1} = (sS_{i+}aA_{i+}cC_{i+}fF_{i+}eE_i) + w\Delta X_t \tag{13}$$

The position vector is calculated as Equation (14):

$$X_{t+1} = X_t + \Delta X_{t+1} \tag{14}$$

A random walk (Lévy flight) is required in order to increase the randomness and improve the stochastic behavior of the artificial dragonflies. Equation (15) is used in order to update the position of dragonflies:

$$X_{t+1} = X_t + Levy(d) \times X_t \tag{15}$$

The Lévy flight is calculated using Equation (16):

$$Levy(x) = 0.01 \times \frac{r_1 \times \sigma}{|r_2|^{\frac{1}{\beta}}} \tag{16}$$

where б is calculated using Equation (17):

$$\sigma = \left(\left(\frac{\Gamma\left(1+\beta\right) \times \sin\left(\frac{\pi\beta}{2}\right)}{\Gamma\left(\frac{1+\beta}{2}\right) \times \beta \times 2^{\left(\frac{\beta-1}{2}\right)}} \right) \right)^{\frac{1}{\beta}} \tag{17}$$

$$\Gamma(x) = (x-1)!$$

The details about DFA are well documented in Refs. [29,30].

DFA variables declaration:

X– Position of current individual
X_j – jth neighboring individual positions
N – Number of neighboring individuals
X^+ – Food source position
X^- – Enemy positions
S_i – Separation of the ith individual
A_i – Alignment of the ith individual
C_i – Cohesion of the ith individual
s – Separation weight
a – alignment weight
c – Cohesion weight
x– Inertia weight
f – Food factor,
e – Enemy factor
t – Iteration count
w – Inertia weight
F_i – Food source of the ith individual
E_i – Position of enemy of the ith individual
d – Dimension of the position vectors
r_1, r_2 – Two random numbers in [0, 1]
β– A constant (equal to 1.5 in this work)

In the proposed approach, the BPNN based model has been driven from BBD experimental matrix and compared with regression modeling results. Next, DF and PSO algorithms have been used to optimize the proposed model (fitness function) by BPNN in such a way that DOP maximized, WBW minimized, and desired ASR achieved simultaneously. As commonly, the architecture of the BPNN is determined based on the trial and error approach, in this study PSO algorithm has been used to determine the proper BPNN architecture and parameters (Tables 5 and 6). Table 7, represents the results of the optimization procedure based on which, DFA could accurately optimize the process responses (with less than 3% error). Fig. 14, illustrates the cross section of weldments for optimized conditions. The convergence of DF and PSO algorithms have been shown in Fig. 15. Apart from using the proposed method for optimization, BBD provides an optimization technique using which ends in quite the same optimization results (Table 7). Fig. 16, represents the optimal levels for the process input parameters in order to obtain the desired output characteristics based on the BBD optimization. DFA.

5. Results and discussion

Different weights (W_1 and W_2) may have been considered for A-GTAW process responses (DOP and WBW) based on the importance considered (Equation (5)). In this study the value of 0.5 has been considered for W_1 and W_2.

In order to attain the best results of using PSO algorithm, three swarm sizes' values (20, 30 and 50) and three iteration numbers (50, 100 and 150) have been used to test the adequacy of the algorithm. The appropriate swarm size value and iterations have been determined 50 and 150 respectively. The best results for determination of parameters c_1 and c_2 and w were 2 and 0.729 respectively. As the same token, Number of artificial dragonflies, max iterations, and max archive size were obtained 500, 150, and 50 respectively.

As per the results of the algorithms (Table 7), it is obvious that the DF algorithm outperforms PSO. Based on the results achieved in this study, the DF algorithm has better efficiency, higher convergence speed, lower computational complexity, better ability to determine the optimal solution. Hence, the DFA is an appropriate algorithm for optimizing the welding process.

6. Conclusion

The problem of modeling and optimization of A-GTAW process for AISI316L austenite stainless steel parts considering both the process input variables and percentage of activating fluxes combination (TiO_2+SiO_2) have been addressed throughout this study. First, Box-behnken design based on response surface methodology has been used to design the experimental tests matrix required for data gathering, modeling, and optimization purposes. Next, DOP and WBW values have been measured using MIP software. Based on the results of WBW and DOP, ASR values have been computed. Then, BPNN and regression modeling have been employed to establish the relations between process input variables (welding speed, current and percentage of activating

Table 7
Optimal A-GTAW process variables and coressponding process measures.

Output	Algorithm	Process variables			Predicted	Experimental	Error (%)
		F	S	C			
$W_{DOP} = 0.50$ and $W_{WBW} = 0.50$							
DOP	DFA-ANN	74	135	100	5.17	5.02	2.90
WBW	DFA-ANN	74	135	100	5.68	5.56	2.11
ASR	DFA-ANN	74	135	100	1.09	1.11	1.01
DOP	PSO-ANN	75	134	100	5.20	5.02	3.40
WBW	PSO-ANN	75	134	100	5.70	5.56	2.60
ASR	PSO-ANN	75	134	100	1.09	1.11	1.11
DOP	BBD	64	131	103	5.00	4.97	0.60
WBW	BBD	64	131	103	6.00	6.20	3.33
ASR	BBD	64	131	103	1.22	1.24	1.68

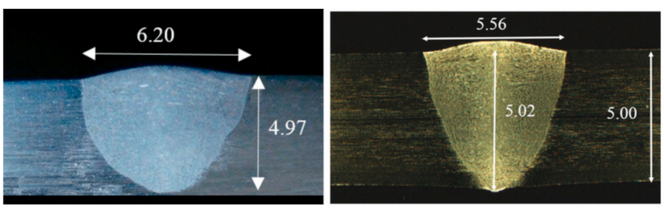

Fig. 14. Evaluation of DOP and WBW for the optimized conditions.

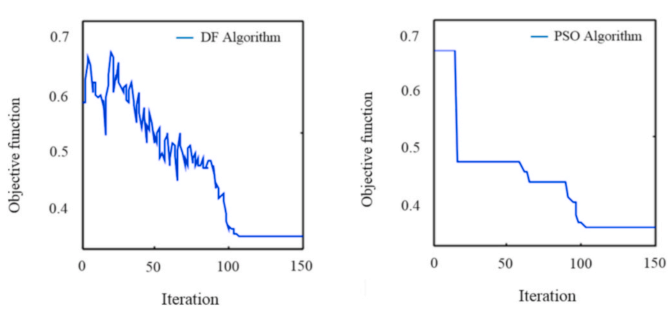

Fig. 15. Convergence of DF and PSO algorithms.

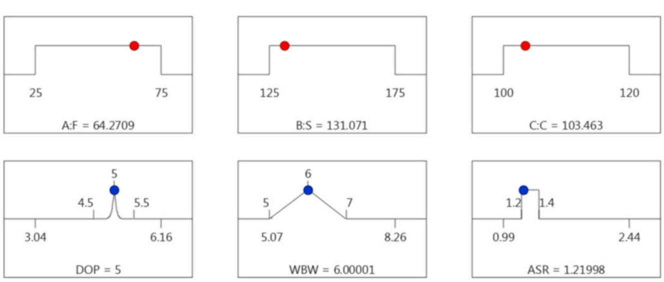

Fig. 16. Optimal process input parameters and their corresponding outputs based on BBD optimization.

fluxes combination) and output responses (DOP, WBW and ASR). Moreover, based on the achieved results, BPNN was more suitable for modeling purpose (less than 3% error) than regression method (about 12% error) based on which BPNN considered as an appropriate tool for modeling purpose. Furthermore, in order to determine the proper BPNN architecture (number of neurons/nodes and hidden layers) PSO algorithm has been used. Then, DF and PSO algorithms have been employed to optimize the proposed BPNN model in such a way that DOP increased, WBW decreased, and desired ASR achieved simultaneously. Based on the optimization results (Table 7), it is clear that the DF algorithm outperforms PSO due to its higher convergence speed and lower computational complexity. Using the proposed hybrid BPNN-DFA approach either process input variables have been optimized (133 mm/s for welding speed and 100 Amp for welding current) and the optimum activating fluxes formula (73% SiO_2 and 27% TiO_2) has been determined in order to achieve the desired process output characteristics (maximum DOP, minimum WBW and desired ASR). The result of proposed optimization procedure showed that the proposed method can precisely simulate and optimize (with less than 3% error) the A-GTAW process.

Author statement

Masoud Azadi Moghaddam: Methodology, Software, Data curation, Writing, Writing – original draft preparation, Visualization, Investigation, Farhad Kolahan: Supervision, Software, Validation, Writing- Reviewing and Editing,

Declaration of competing interest

The authors declare that they have no known competing financial interests or personal relationships that could have appeared to influence the work reported in this paper.

References

[1] R.S. Vidyarthy, A. Kulkarni, D.K. Dwivedi, Study of microstructure and mechanical property relationships of A-TIG welded P91-316L dissimilar steel joint, Mater. Sci. Eng. 695 (2017) 249–257.
[2] K.D. Ramkumar, V. Varma, M. Prasad, N.D. Rajan, Effect of activated flux on penetration depth, microstructure and mechanical properties of Ti-6Al-4V TIG welds, J. Mater. Process. Technol. 261 (2018) 233–241.
[3] Y. Zou, R. Ueji, H. Fujii, Mechanical properties of advanced active- TIG welded duplex stainless steel and ferrite steel, Mater. Sci. Eng. 620 (2015) 140–148.
[4] A. Kulkarni, D.K. Dwivedi, M. Vasudevan, Dissimilar metal welding of P91 steel-AISI 316L SS with Inconel 800 and Inconel 600 interlayers by using activated TIG welding process and its effect on the microstructure and mechanical properties, J. Mater. Process. Technol. 274 (2019) 116–128.
[5] R.S. Vidyarthy, D.K. Dwivedi, Microstructural and mechanical properties assessment of the P91 A-TIG weld joints, J. Manuf. Process. 31 (2018) 523–535.
[6] K.H. Dhandha, V.J. Badheka, Effect of activating fluxes on weld bead morphology of P91 steel bead-on-plate welds by flux assisted tungsten inert gas welding process, Mater. Manuf. Process. 17 (2015) 48–57.
[7] R. Pamnani, M. Vasudevan, P. Vasantharaja, T. Jayakumar, Optimization of A-GTAW parameters for naval steel (DMR 249 A) by design of experiments approach, J. Mater. Design Appl. 34 (2015) 1–12.
[8] B. Arivazhagan, M. Vasudevan, Studies on A-TIG welding of 2.25 Cr–1Mo (P22) steel, Mater. Manuf. Process. 18 (2015) 55–59.
[9] B. Arivazhagan, M. Vasudevan, A comparative study on the effect of GTAW processes on the microstructure and mechanical properties of P91 steel weld joints, Mater. Manuf. Process. 16 (2014) 305–311.
[10] E. Ahmadi, A.R. Ebrahimi, Welding of 316L austenitic stainless steel with activated tungsten inert gas process, J. Mater. Eng. Perform. 24 (2015) 1065–1071.
[11] M. Kurtulmus, Effects of welding parameters on penetration depth in mild steel A-TIG welding, Sci. Iran. B 26 (2019) 1400–1404.
[12] V.B. Kumar, D. Lucas, G. Howse, S. Melton, L. Raghunathan, G. Vilarinho, Investigation of the A-TIG mechanism and the productivity benefits in TIG welding, Fifteenth International Conference on the Joining of Materials 15 (December) (2009).

[13] G. Venkatesan, J. George, M. Sowmyasri, V. Muthupandi, Effect of ternary fluxes on depth of penetration in A-TIG welding of AISI 409 ferritic stainless steel, Proced. Mater. Sci. 5 (2014) 2402–2410.
[14] T.S. Chern, K.H. Tseng, H.L. Tsai, Study of the characteristics of duplex stainless steel activated tungsten inert gas welds, M*ater. Des.* 32 (2011) 255–263.
[15] S. Tathgir, A. Bhattacharya, Activated-TIG welding of different steels: influence of various flux and shielding gas, Mater. Manuf. Process. 31 (2015) 335–342.
[16] V.M. Martínez, F.J. Gomez-Gil, J. Gomez-Gil, F. Ruiz-Gonzalez, An artificial neural network based expert system fitted with genetic algorithms for detecting the status of several rotary components in agro-industrial machines using a single vibration signal, Expert Syst. Appl. 42 (2015) 6433–6441.
[17] A.P. Markopoulos, D.E. Manolakos, N.M. Vaxevanidis, Artificial neural network models for the prediction of surface roughness in electrical discharge machining, J. Intel. Manuf. 12 (2008) 283–292.
[18] H. Sahin, B. Topal, Impact of information technology on business performance: integrated structural equation modelling and artificial neural network approach, Sci. Iran. B 25 (2018) 1272–1280.
[19] M. Kurtulmus, A. Kiraz, Artificial neural network modelling for polyethylene FSSW parameters, Sci. Iran. B 25 (2018) 1266–1271.
[20] N. Gregory, Why do welds crack? TWI Bull March/April (1991) 1–8.
[21] R. Pamnani, M. Vasudevan, P. Vasantharaja, T. Jayakumar, Optimization of A-GTAW welding parameters for naval steel (DMR 249 A) by design of experiments approach, J. Mater.: Design and Applications 12 (2015) 1–12.
[22] M.H.M.A. Jahromi, R. Tavakkoli Moghaddam, A. Makui, A. Shamsi, Solving a one-dimensional cutting stock problem by simulated annealing and tabu search, J. Indus. Eng. Int. 8 (2012) 1–8.
[23] M.A. Ayubi Rad, M.S. Ayubi Rad, Comparison of artificial neural network and coupled simulated annealing based least square support vector regression models for prediction of compressive strength of high-performance concrete, Sci. Iran. 24 (2017) 487–496.
[24] K.H. Lee, K.W. Kim, Performance comparison of particle swarm optimization and genetic algorithm for inverse surface radiation problem, Int. J. Heat Mass Tran. 88 (2015) 330–337.
[25] K. Zhi, W. Jia, G. Zhang, L. Wang, Normal parameter reduction in soft set based particle swarm optimization algorithm, Appl. Math. Model. 39 (2015) 4808–4820.
[26] M. Azadi Moghaddam, F. Kolahan, Using Combined Artificial Neural Network and Particle Swarm Optimization Algorithm for Modeling and Optimization of Electrical Discharge Machining Process, S*cientia Iranica B*, 2018 in press.
[27] M.M. Hasheminejad, N. Sohankar, A. Hajiannia, Predicting the collapsibility potential of unsaturated soils using adaptive neural fuzzy inference system and particle swarm optimization, Sci. Iran. 25 (2018) 2980–2996.
[28] M. Azadi Moghaddam, R. Golmezergi, F. Kolahan, Multi-variable measurements and optimization of GMAW parameters for API-X42 steel alloy using a hybrid BPNN–PSO approach, Measurement 92 (2016) 279–287.
[29] Pitchipoo, P.; Muthiah, A.; Jeyakumar, K.; Manikandan, A. Friction stir welding parameter optimization using novel multi objective dragonfly algorithm. Int. J. Lightweight Mater. Manuf., https://doi.org/10.1016/j.ijlmm. 2021.06.006.
[30] Mirjalili, S. Dragonfly algorithm: a new meta-heuristic optimization technique for solving single-objective, discrete, and multi-objective problems. Neural Comput. Appl., DOI 10.1007/s00521-015-1920-1.